Mechanism of Alkane C−H Bond Activation by Copper and Silver Homoscorpionate Complexes

Ataualpa A. C. Braga,[†] Feliu Maseras,*[,†] Juan Urbano,[‡] Ana Caballero,[‡] M. Mar Díaz-Requejo,*[,‡] and Pedro J. Pérez*[,‡]

Institute of Chemical Research of Catalonia (ICIQ), Avgda. Països Catalans, 16, 43007 Tarragona, Catalonia, Spain, and Laboratorio de Catálisis Homogénea, Departamento de Química y Ciencia de los Materiales, Unidad Asociada al CSIC, Universidad de Huelva, Campus de El Carmen, 21007 Huelva, Spain

Received May 21, 2006

DFT Becke3LYP calculations are applied to the computational study of the activation of alkane C−H bonds by metallocarbene homoscorpionate complexes. A total of 16 different combinations of metallocarbene complex and alkane are explored, defined by the use of $TpAg{=}C(H)(CO_2CH_3)$, $Tp^{Br3}Ag{=}C(H)(CO_2CH_3)$, $TpCu{=}C(H)(CO_2CH_3)$, and $Tp^{Br3}Cu{=}C(H)(CO_2CH_3)$ species as metallocarbene and methane, ethane, propane, and butane as alkane. The reaction is found to be under kinetic control, and the selectivity is decided in a step with a low-barrier transition state where the key bond-breaking and bond-forming processes take place in a concerted way. This transition state has several possible conformations, which are systematically explored to find the one with lowest energy for each reaction. Variations of the energy barrier as a function of the nature of metal, ligand, and alkane are analyzed and discussed.

Introduction

The development of selective and efficient methods to activate C−H bonds still remains a difficult task despite the great advances produced in the area of organometallic chemistry in the past decades. The interest in the topic is due to the ready availability of hydrocarbon resources and the interest in the synthesis of value-added compounds from simple precursors.[1]

The metal-catalyzed carbene insertion into unactivated C−H bonds, using diazo compounds as the carbene source, is an emerging tool for alkane activation.[2] This process consists of two steps: (i) generation of a very reactive metallocarbene intermediate $L_nM{=}C(R^1)(R^2)$, from the reaction of the metal catalyst and the diazocompound (Figure 1, eq 1), and (ii) carbene insertion into the C−H bond and release of the initial metal complex to start the catalytic cycle (Figure 1, eq 2). The mechanism of the reaction between metallocarbene and alkane has been investigated by experimental[3] and theoretical methods[4] for the case of dirhodium(II) tetracarboxylate complexes. The rate-determining step of the whole process is the formation of the metallocarbene species,[2,5] but the nature of the C−H bond being activated is decided in the carbene insertion step, by means of a concerted mechanism.

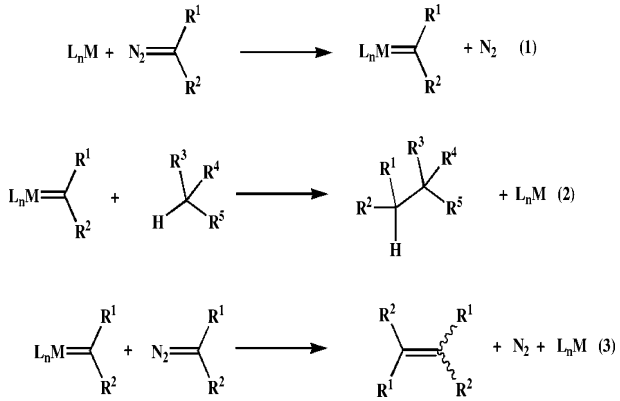

Figure 1. Metal-catalyzed transfer of carbene units from diazo compounds: formation of metallocarbene (eq 1), insertion into C−H bonds (eq 2), and formation of olefin byproducts (eq 3).

In the last years, it has been shown by us[6−9] and others[10] that the product from the reaction between Tp^xML (M = Cu, Ag; Tp^x = trispyrazolylborate ligand; L = leaving group) and ethyl diazoacetate (EDA) catalyzes the insertion of the $:CHCO_2Et$ unit, from EDA, into a variety of alkane C−H bonds. These studies have shown that (i) silver-based catalysts species

* Corresponding authors. E-mail: fmaseras@iciq.es; perez@dqcm.uhu.es.
[†] ICIQ.
[‡] Universidad de Huelva.

(1) (a) Labinger, J. A.; Bercaw, J. E. *Nature* **2002**, *417*, 507. (b) Shilov, A. E.; Shulpin, G. B. *Activation and Catalytic Reactions of Saturated Hydrocarbons in the Presence of Metal Complexes*; Kluwer: Dordrecht, 2000. (b) Dyker, G. *Angew. Chem., Int. Ed. Engl.* **1989**, *28*, 1698. (c) Guari, Y.; Sabo-Etienne, S.; Chaudret, B. *Eur. J. Inorg. Chem.* **1999**, 1047. (d) Shilov, A. E.; Shulpin, G. B. *Chem. Rev.* **1997**, *97*, 2879. (e) Arndtsen, B. A.; Bergman, R. G.; Mobley, T. A.; Peterson, T. H. *Acc. Chem. Res.* **1995**, *28*, 154.

(2) (a) Davies, H. M. L.; Beckwith, R. E. J. *Chem. Rev.* **2003**, *103*, 2861. (b) Doyle, M. P.; McKervey, M. A.; Ye, T. *Modern Catalytic Methods for Organic Synthesis with Diazo Compounds*; John Wiley & Sons: New York, 1998. (c) Doyle, M. P. In *Comprehensive Organometallic Chemistry II*; Abel, E. W., Stone, F. G. A., Wilkinson, G., Eds.; Pergamon Press: Oxford, U.K., 1995; Vol. 12, p 421.

(3) Pirrung, M. C.; Liu, H.; Morehead, A. T. *J. Am. Chem. Soc.* **2002**, *124*, 1014.

(4) Nakamura, E.; Yoshikai, N.; Yamanaka, M. *J. Am. Chem. Soc.* **2002**, *124*, 7181.

(5) Kirmse, W. *Angew. Chem., Int. Ed.* **2003**, *42*, 1088.

(6) Díaz-Requejo, M. M.; Belderraín, T. R.; Nicasio, M. C.; Trofimenko, S.; Pérez, P. J. *J. Am. Chem. Soc.* **2002**, *124*, 896.

(7) Caballero, A.; Díaz-Requejo, M. M.; Belderraín, T. R.; Nicasio, M. C.; Trofimenko, S.; Pérez, P. J. *J. Am. Chem. Soc.* **2003**, *125*, 1446.

(8) Caballero, A.; Díaz-Requejo, M. M.; Belderraín, T. R.; Nicasio, M. C.; Trofimenko, S.; Pérez, P. J. *Organometallics* **2003**, *22*, 4145.

(9) Urbano, J.; Belderraín, T. R.; Nicasio, M. C.; Trofimenko, S.; Díaz-Requejo, M. M.; Pérez, P. J. *Organometallics* **2005**, *24*, 1528.

(10) (a) Dias, H. V. R.; Browning, R. G.; Richey, S. A.; Lovely, C. J. *Organometallics* **2004**, *23*, 1200. (b) Dias, H. V. R.; Browning, R. G.; Richey, S. A.; Lovely, C. J. *Organometallics* **2005**, *24*, 5784.

10.1021/om060445h CCC: $33.50
Publication on Web 09/21/2006

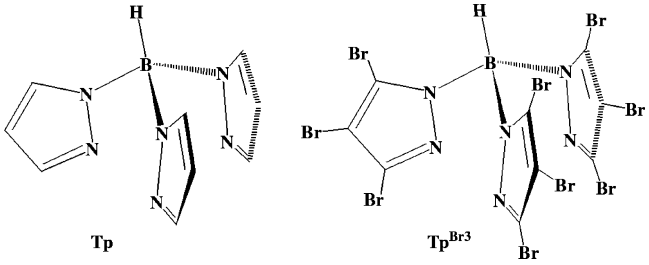

Figure 2. Tp and Tp^{Br3} ligands.

are more reactive than those with copper and (ii) there is also a defined trend in the reactivity of the C−H bonds, always in the order tertiary > secondary > primary. This behavior is in agreement with what one would expect from the sequence of C−H bond energies. A nondesired side reaction very often competes with this process, corresponding to the reaction of the metallocarbene complex with a second molecule of EDA to give diethyl fumarate and maleate (Figure 1, eq 3).

The selectivities observed with these catalysts depended on the nature of the metal and the ligand employed. The design of more efficient catalysts would largely benefit from a better understanding of the reaction mechanism. However, the reaction of the alkane and EDA in the presence of these copper catalysts is so fast that intermediates cannot be isolated; therefore the nature of the metallocarbene complex itself is not yet understood. In this contribution, we report a computational study on the mechanism of this metal-catalyzed carbene insertion reaction. The carbene unit used is the :$CHCO_2Me$ fragment, very similar to the experimental system (:$CHCO_2Et$), but easier to compute in terms of conformational complexity. A total of four metal fragments are considered, TpAg, Tp^{Br3}Ag, TpCu, and Tp^{Br3}Cu, resulting from the combination of the two metal atoms experimentally applied and of two Tp ligands (Figure 2). These are Tp itself, because of formal simplicity and small size, and Tp^{Br3},[7−9] because of its experimental efficiency. Four different substrates are used for C−H activation: H_3C−H, $(CH_3)H_2C$−H, $(CH_3)_2HC$−H, and $(CH_3)_3C$−H. These compounds are the simplest examples of saturated C−H bonds on primary, secondary, and tertiary sites.

Computational Details

Calculations were performed at the DFT level, by means of the Becke3LYP[11−13] functional, with a hybrid Becke3 exchange functional and a Lee−Yang−Parr correlation functional[11,12] using the Gaussian suite of programs.[14] Cu, Ag, and Br atoms were described using an effective core potential (LANL2DZ) for the inner electrons[14,15] and its associated double-ζ basis set for the outer ones. An additional f polarization shell was added for Cu and Ag, with exponents of 3.525 and 1.611, respectively.[16] In the case of Br, a d polarization shell was added (exponent 0.4280).[17] The 6-31G(d) basis set was used for the H, B, C, N, and O atoms.[18] The structures

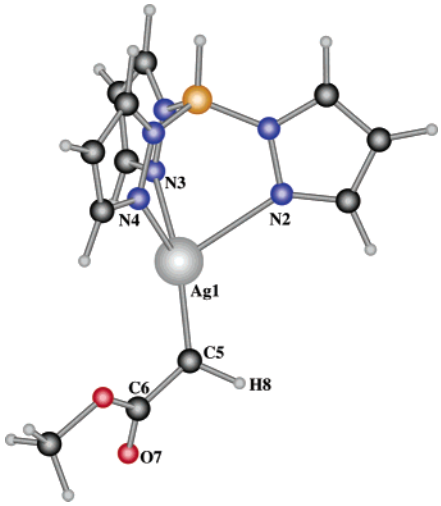

Figure 3. TpAg=C(H)(CO_2CH_3) carbene complex.

of the reactants, intermediates, transition states, and products were fully optimized without any symmetry restriction. Transition states were identified by having one negative eigenvalue in the Hessian matrix. Solvation effects were introducted using single-point PCM[19] calculations on gas-phase optimized geometries. A temperature of 25 °C was assumed in the calculation of free energy corrections.

The calculations must be able to reproduce the small energy differences associated with the low experimental selectivities. These have been postulated to correlate with differences in the C−H bond dissociation energy of the different alkanes, which in turn are also known to be small. To estimate the accuracy of our method for this problem, we carried out a series of calculations on the homolytic cleavage of the C−H bond of the alkanes being analyzed, namely, H_3C−H, $(CH_3)H_2C$−H, $(CH_3)_2HC$−H, and $(CH_3)_3C$−H. With the Becke3LYP computational method described above, the potential energy costs for these dissociation processes are 112.9, 108.2, 104.1, and 100.6 kcal/mol, respectively. The same calculations were repeated with a more accurate CCSD(T) approach, and the results were 104.5, 101.3, 98.5, and 96.3 kcal/mol. The difference in absolute cost for the bond cleavage is as large as 8.4 kcal/mol for the case of H_3C−H, but results are better for the relative strength of the bonds. The ordering of energies is perfectly reproduced, and the differences between the alkanes are comparable. Becke3LYP has been shown to be quite accurate before for this type of process.[20]

Results

Reaction of TpAg=C(H)(CO_2CH_3) with Ethane. Starting Carbene Complex. Figure 3 presents the optimized geometry of the metallocarbene complex TpAg=C(H)(CO_2CH_3). The short Ag1−C5 distance of 2.026 Å combined with the Ag1−C5−C6 and Ag1−C5−H8 bond angles of 127.1° and 120.5°, respectively, are consistent with the presence of a carbene ligand. The three substituents around the C5 carbene atom are in a planar arrangement, with a value of 193.8° for the H8−C5−Ag1−C6 dihedral angle. The ester group is tilted with respect to the carbene plane, and the Ag1−C5−C6−O7 dihedral angle is 120.4°, far from the 180° expected for a coplanar arrangement. The Tp ligand stays in a tricoordinate arrangement that is quite asymmetric, with Ag1−N2, Ag1−N3, and Ag1−N4 distances of 2.513, 2.244, and 2.334 Å, respectively. The orientation of the carbene substituents with respect to the Ag−N bonds can be a source of conformational complexity. This orientation is neither staggered nor eclipsed (the N2−Ag1−C5−C6 dihedral

(11) Lee, C.; Parr, R. G.; Yang, W. *Phys. Rev. B* **1988**, *37*, 785.
(12) Becke, A. D. *J. Chem. Phys.* **1993**, *98*, 5648.
(13) Stephens, P. J.; Devlin, F. J.; Chabalowski, C. F.; Frisch, M. J. *J. Phys. Chem.* **1994**, *98*, 11623.
(14) Frisch, M. J.; et al. *Gaussian 03*, Revision C.02; Gaussian, Inc.: Wallingford, CT, 2004.
(15) Wadt, W. R.; Hay, P. J. *J. Chem. Phys.* **1985**, *82*, 284.
(16) Ehlers, A. W.; Böhme, M.; Dapprich, S.; Gobbi, A.; Höllwarth, A.; Jonas, V.; Köhler, K. F.; Stegmann, R.; Veldkamp, A.; Frenking, G. *Chem. Phys. Lett.* **1993**, *208*, 111.
(17) Höllwarth, A.; Böhme, M.; Dapprich, S.; Ehlers, A. W.; Gobbi, A.; Jonas, V.; Köhler, K. F.; Stegmann, R.; Veldkamp, A.; Frenking, G. *Chem. Phys. Lett.* **1993**, *208*, 237.
(18) Francl, M. M.; Pietro, W. J.; Hehre, W. J.; Binkley, J. S.; Gordon, M. S.; Defrees, D. J.; Pople, J. A. *J. Chem. Phys.* **1982**, *77*, 3654.
(19) Miertus, S.; Scrocco, E.; Tomasi, J. *Chem. Phys.* **1981**, *55*, 117.
(20) Vreven, T.; Morokuma, K. *J. Chem. Phys.* **1999**, *111*, 8799.

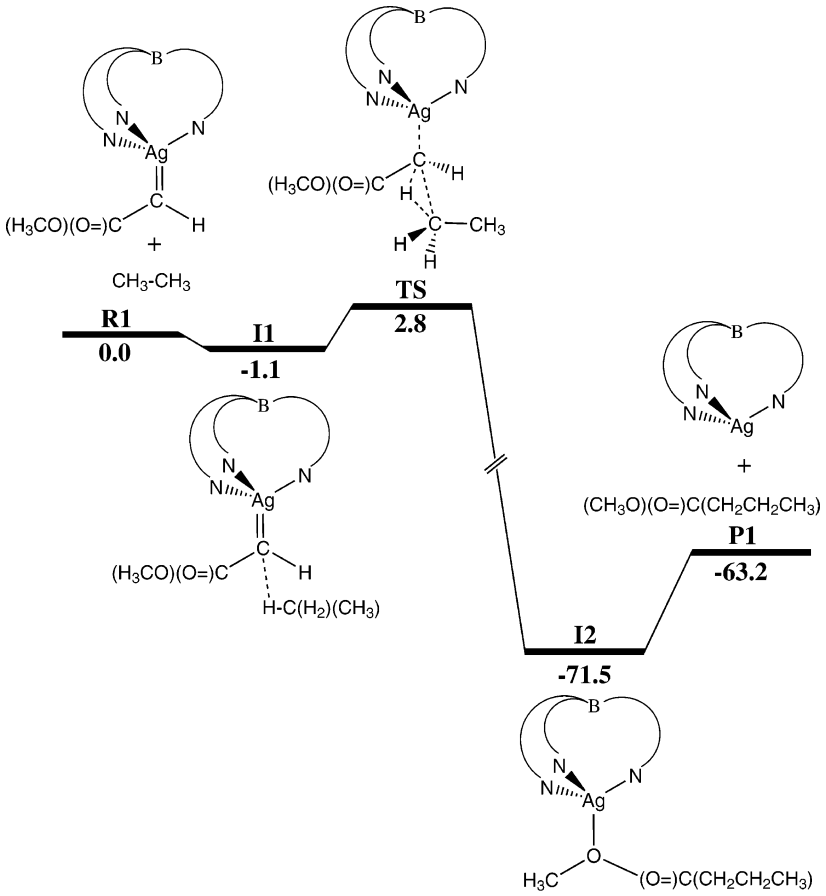

Figure 4. Energy profile (in kcal/mol) of a reaction path for the reaction between TpAg=C(H)(CO_2CH_3) and ethane.

angle is 208.6°), and different possible placements of the longer Ag−N2 bond with respect to the C6 carbon center can be viewed. The geometry presented in Figure 3 is the only we could find to be a local minimum. It has a transoid arrangement between C6 and N2, the value of 208.6° being closer to 180° than to 0°.

Plausible Reaction Path. Figure 4 presents an energy profile for the insertion of the :$CHCO_2Me$ carbene ligand of TpAg=C(H)(CO_2CH_3) into one of the C−H bonds of ethane. The initial approach between the two reactants produces intermediate **I1**, shown in Figure 5. There is a weak interaction between both species, as shown by the small stabilization energy of 1.1 kcal/mol. The shortest distance between the two fragments corresponds to the 2.877 Å of O14···H9 distance. The interaction between ethane and the C5 carbene atom is very weak, and the C5···H9 distance is 3.413 Å.

The reaction continues through transition state **TS1**, also in Figure 5. In the step associated with this transition state, the insertion of the carbene atom C5 in the C10−H9 bond takes place. The transition vector associated with the single imaginary frequency shows that the formation of the C5−C10 and C5−H9 chemical bonds is coupled with the breaking of the Ag1−C5 and C10−H9 bonds in this transition state. The values for all these bond distances are reasonable. The distances for the forming C5−H9 and C5−C10 bonds are 1.323 and 2.371 Å, respectively, whereas the corresponding values for the breaking bonds C10−H9 and Ag1−C5 are 1.225 and 2.153 Å. This transition state has a low barrier; it is only 3.9 kcal/mol above intermediate **I1** and 2.8 kcal/mol above the separate reactants.

Transition state **TS1** evolves to intermediate **I2**, also in Figure 5. In this species, the $CH_3CO_2(CH_2)_2CH_3$ product is already formed, but stays bound to the silver center through the ester oxygen O14. The Ag1−O14 distance is as long as 2.476 Å. The overall reaction is very exothermic; **I2** is 71.5 kcal/mol

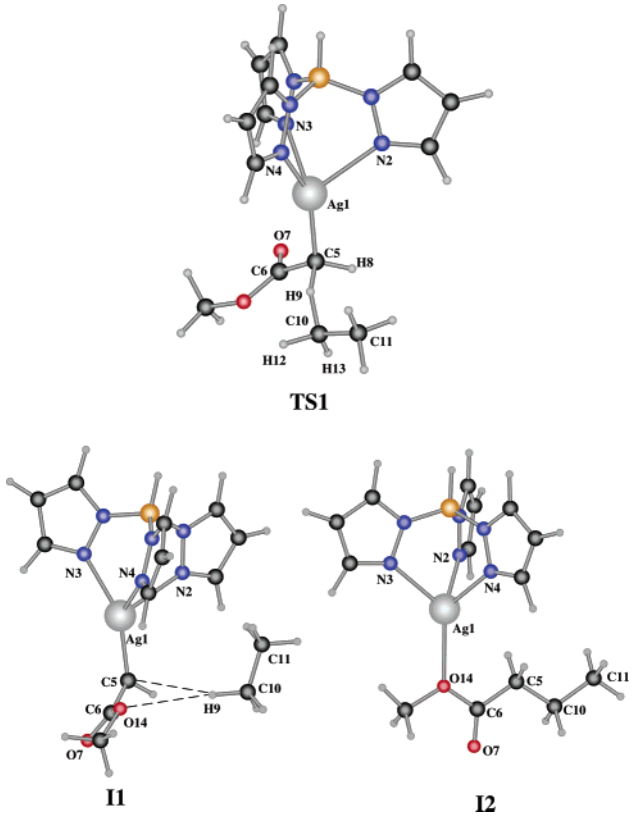

Figure 5. Geometries of stationary points along the reaction path for the reaction between TpAg=C(H)(CO_2CH_3) and ethane.

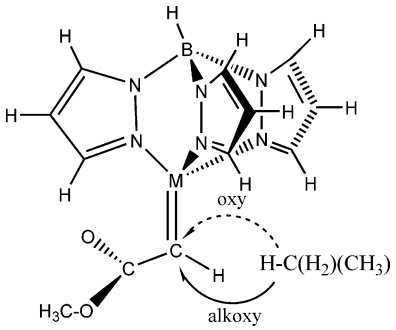

Figure 6. Possible approaches of alkane to carbene through the oxy or alkoxy faces.

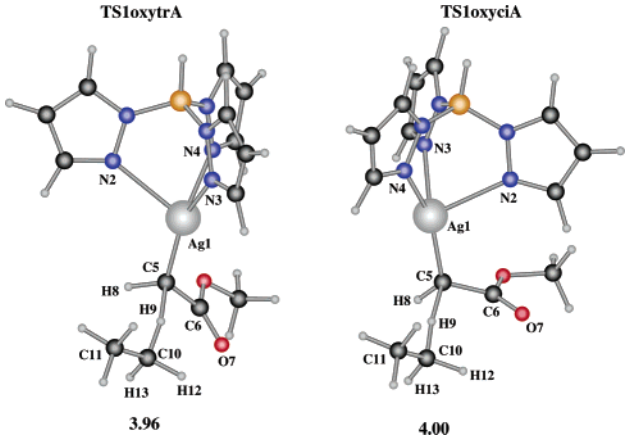

Figure 7. Optimized Becke3LYP structures of conformers **TS1oxytrA** and **TS1oxyciA** of the transition state for the reaction between TpAg=C(H)(CO_2CH_3) and ethane. Relative energies with respect to separate reactants are given in kcal/mol.

below the separate reactants and 74.3 kcal/mol below **TS1**. The last point in Figure 4 corresponds to the separate products, with an energy of 8.3 kcal/mol above **I2**. This 8.3 kcal/mol value corresponds to the coordination energy of $CH_3CO_2(CH_2)_2CH_3$ to the TpAg complex.

The key species in the reaction profile is clearly **TS1**, which corresponds to a highly irreversible step where furthermore the stereoselectivity of the products is decided. Consequently, most of the discussion in this article will focus on the relative energies of these type of transition states. **TS1** has several possible conformations for the particular combination of the TpAg=C(H)(CO_2CH_3) metallocarbene and ethane, as discussed below.

Oxy Face or Alkoxy Face. The direction from which the ethane molecule approaches the carbene can give rise to different conformers. The ethane may approach the planar carbene center from one of the two sides, which are not equivalent because of the arrangement of the ester group. In the isolated carbene complex, the ester plane is nearly perpendicular with the carbene plane and, as a result, one of the faces contains the carbonyl oxygen, while the other one contains the alkoxy group, as indicated schematically in Figure 6.

The plausible mechanism presented above corresponds to the alkoxy face, and the corresponding structures will be referred to in what follows with the **alk** label, that is, **I1alk**, **TS1alk**, and **I2alk**. We were able to locate also the analogous saddle point **TS1oxy**, corresponding to an approach through the oxy face. Its geometry is shown in Figure 7 with the label **TS1oxytrA**, and selected geometrical parameters are included in Table 1, together with those of other structures. The comparison between structures **TS1alktrA** and **TS1oxytrA** shows that the difference in the face of attack is reflected in the O7−C6−C5−H9 dihedral angle, with a value of 187.5° (close to 180°) for **TS1alktrA** and a value of 9.6° (close to 0°) for **TS1oxytrA**. It is also worth noting that the transition state seems to be earlier when the reaction takes place through the oxy face; the C5−H9 and C5−C10 distances are 1.582 and 2.655 Å, compared to values of 1.323 and 2.371 Å for the alkoxy face. The energy of **TS1oxy** with respect to the separate reactants is 4.0 kcal/mol, thus 1.2 kcal/mol above that of **TS1alk**. The oxy face is thus not preferred for this particular couple of metal complex and alkane.

Tp Arrangement. It has been mentioned above that for the starting complex only the conformation with the transoid arrangement between the C6−C5 and Ag1−N2 bonds was possible. This is no longer the case for the transition states. The structures presented above have transoid arrangements and will be thus labeled as **TS1alktr** and **TS1oxytr**, but another saddle point, **TS1oxyci**, could be also optimized, its geometry being shown in Figure 7. Geometrical parameters for **TS1oxyci** are similar to those for **TS1oxytr**, with the clear exception of the N2−Ag1−C5−C6 dihedral angle, which is 222.9° for the transoid structure and 46.1° for the cisoid one. The difference in the relative energies of both saddle points is negligible, with **TS1oxyci** 0.04 kcal/mol above **TS1oxytr**. This has no chemical relevance, since both are higher in energy than **TS1alktr**, which has been reported above. The cisoid equivalent of **TS1alktr** could not be optimized: the calculation always went to the transoid conformer.

Three Possible Ethyl Orientations. The orientation of the ethane molecule approaching the starting carbene species is an additional source of conformational complexity. Apart from the H9 atom belonging to the C10−H9 bond being broken, C10 has three other substituents, one methyl and two hydrogens. These substituents can be arranged in different ways, giving rise to the three conformations, which are labeled arbitrarily as **A**, **B**, and **C**. Figure 8 shows the three structures for the particular case of an approach to the alkoxy face of a complex

Table 1. Selected Geometrical Parameters (Å and deg) and Relative Energies (kcal/mol) for Conformers of the Transition State for the Reaction between TpAg=C(H)(CO_2CH_3) and Ethane

	TS1alktr			TS1alkci		TS1oxytr			TS1oxyci		
	A	B	C	B	C	A	B	C	A	B	C
C5−H9	1.323	1.307	1.261	1.323	1.269	1.582	1.598	1.407	1.641	1.657	1.479
C10−H9	1.225	1.233	1.263	1.221	1.254	1.149	1.148	1.189	1.140	1.139	1.168
C5−C10	2.371	2.356	2.327	2.372	2.320	2.655	2.671	2.522	2.732	2.728	2.602
Ag1−C5	2.153	2.163	2.178	2.166	2.189	2.080	2.078	2.113	2.072	2.070	2.098
Ag1−N2	2.500	2.489	2.468	2.508	2.479	2.542	2.544	2.534	2.556	2.557	2.548
Ag1−N3	2.368	2.371	2.391	2.404	2.426	2.293	2.295	2.357	2.329	2.313	2.350
Ag1−N4	2.341	2.352	2.352	2.334	2.345	2.343	2.336	2.317	2.287	2.302	2.299
C5−H9−C10−C11	112.6	209.3	349.6	207.6	336.0	120.6	224.2	16.0	160.7	230.4	3.7
N2−Ag1−C5−C6	222.9	219.7	229.1	46.1	53.0	212.3	209.3	211.8	11.2	13.2	347.0
O7−C6−C5−H9	187.5	188.9	188.8	193.5	192.0	9.6	13.7	12.6	23.5	25.9	338.2
energy	2.8	2.9	4.7	3.1	5.2	4.0	3.7	4.5	4.0	3.5	4.4

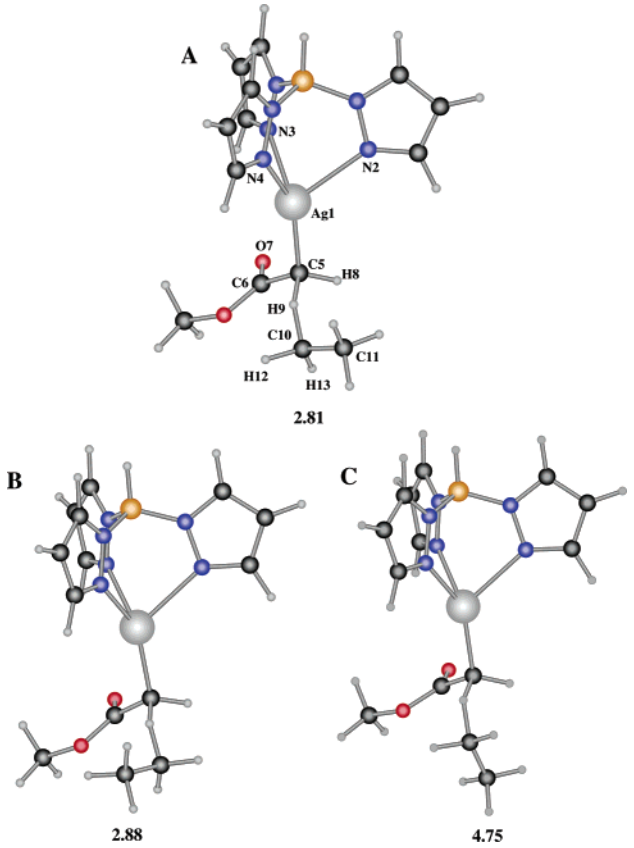

Figure 8. Optimized Becke3LYP structures of conformers **TS1alktrA**, **TS1alktrB**, and **TS1alktrC** of the transition state for the reaction between TpAg=C(H)(CO_2CH_3) and ethane. Relative energies with respect to separate reactants are given in kcal/mol.

with a transoid arrangement: **TS1alktrA**, **TS1alktrB**, and **TS1alktrC**. **TS1alktrA** corresponds to the structure presented above as **TS1** in Figure 4, and it is the lowest energy saddle point and thus the true transition state of the reaction.

A similar set of three rotamers can be found for the transition states of most of the other three combinations of face of attack and Tp arrangement: **alkci**, **oxytr**, **oxyci**. Their structures are given in the Supporting Information, and selected geometrical parameters and relative energies are given in Table 1. The main differences between the reported parameters correspond to the definition of the distinct pathways. **alk**, **oxy** structures differ in the O7−C6−C5−H9 dihedral angle; **ci**, **tr** structures differ in the N2−Ag1−C5−C6 dihedral angle; and **A**, **B**, **C** structures differ in the C5−H9−C10−C11 dihedral angle. It is worth noticing that the four key bond distances C5−H9, C10−H9, C5−C10, and Ag1−C5, related to the bonds being broken and formed, are quite independent of the **A**, **B**, and **C** ethyl orientation. The values for the C5−H9 distance in the five geometries sharing the **TS1alk** label are between 1.323 and 1.269 Å. **TS1oxy** structures present values between 1.407 and 1.598 Å, with a larger dispersion, although the interactions are obviously weaker, and thus energies are less sensitive to geometrical changes.

The relative energies of the saddle points are between a lowest value of 2.8 kcal/mol for **TS1alktrA** and a highest value of 5.2 kcal/mol for **TS1oxytrC**. All these values correspond to feasible processes, but it is chemically relevant to identify the saddle point with the lowest energy, because the choice of the correct value of the barrier can be critical for a computational estimation of the selectivity.

Table 2. Relative Energies (kcal/mol) for Stationary Points in the Lowest Energy Pathways for C−H Activation of Different Alkanes by TpAg=C(H)(CO_2CH_3)

	I1	**TS1**	**I2**	**P1**	barrier
$(H)_3C-H$	−0.4	7.4	−70.3	−61.8	7.8
$(CH_3)(H)_2C-H$	−1.1	2.8	−71.5	−63.1	3.9
$(CH_3)_2(H)C-H$	−1.3	0.0	−71.7	−64.1	1.3
$(CH_3)_3C-H$	−1.3	−0.8	−70.2	−62.6	0.5

Table 3. Selected Geometrical Parameters (Å and deg) for the Transition States Associated with the Lowest Energy Pathway for C−H Activation of the Different Alkanes by TpAg=C(H)(CO_2CH_3)

	CH_4	C_2H_6	C_3H_8	C_4H_{10}
	alktrA	**alktrA**	**alktrA**	**alktrA**
C5−H9	1.298	1.323	1.722	2.002
C10−H9	1.238	1.225	1.134	1.118
C5−C10	2.251	2.371	2.835	3.101
Ag1−C5	2.182	2.153	2.074	2.050
Ag1−N2	2.472	2.500	2.562	2.574
Ag1−N3	2.373	2.368	2.356	2.336
Ag1−N4	2.351	2.341	2.294	2.279
C5−H9−C10−X11	105.7	112.6	69.9	44.7
N2−Ag1−C5−C6	222.4	222.9	182.8	179.8
O7−C6−C5−H9	184.8	187.5	199.5	203.6
energy	7.4	2.8	0.0	−0.8

Reaction of TpAg=C(H)(CO_2CH_3) with Methane, Propane, and Butane. The pattern of the reaction of TpAg=C(H)(CO_2CH_3) with the other alkanes considered is similar to that of ethane. It is a smooth reaction profile, with an early low-energy transition state, and there are a variety of conformers of this transition state. They have been systematically searched for methane, propane, and butane, and the energetics for the stationary points connected to the lowest energy paths are collected in Table 2.

Table 2 includes in the last column the barrier for the chemical reaction, corresponding to the energy difference between **TS1** and the starting intermediate **I1**. The barrier diminishes in the series methane, ethane, propane, butane, with values of 7.8, 3.9, 1.3, and 0.5 kcal/mol, respectively. This is in good agreement with the experimental observation that the C−H bonds associated with the more substituted carbons are easier to activate,[9] a result that is attributed to the different bond dissociation energies of the C−H bonds. It is worth mentioning that the table shows that the experimentally observed preference for activation of more substituted alkanes is due to kinetic control, because thermodynamics would point otherwise. If we look at the energy of products **P1** with respect to the reactants, we can see that in the case of butane the reaction is less exothermic than for ethane or propane.

The fact that all C−H activation barriers are quite low may lead to the wrong conclusion that this complex should activate all alkanes, in contradiction with the experimental observation. This reasoning would neglect the role of competing reactions, which can prevent activation. It has been explained that EDA also undergoes metal-catalyzed decomposition to give diethyl fumarate (DEF) and maleate (DEM). The barrier for this process, not computed in this work, would mark an upper barrier limit for the C−H activation process to be efficient. Above this limit, the metallocarbene would afford DEM and DEF before reacting with the C−H bond. The fact that **TS1** has an energy below the reactants in the case of $(CH_3)_3C-H$ has no special significance. It responds only to the presence of a relatively stable **I1** intermediate coupled with a very low energy barrier.

Data in Table 3 correspond in all cases to the lowest energy paths, and their determination has required calculations on a

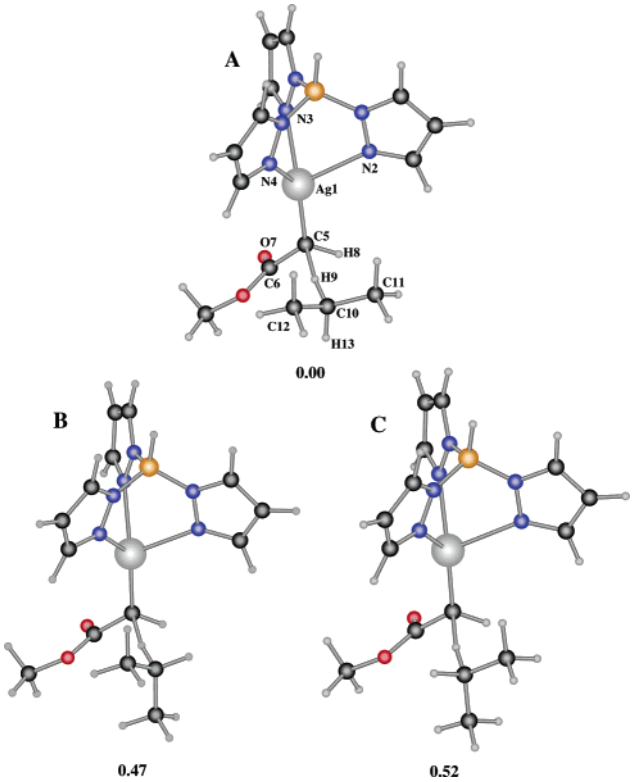

Figure 9. Optimized Becke3LYP structures of conformers **TS1alktrA**, **TS1alktrB**, and **TS1alktrC** of the transition state for the reaction between $TpAg{=}C(H)(CO_2CH_3)$ and propane. Relative energies with respect to separate reactants are given in kcal/mol.

Table 4. Relative Energies (kcal/mol) for Stationary Points in the Lowest Energy Pathways for C−H Activation of Different Alkanes by $Tp^{Br3}Ag{=}C(H)(CO_2CH_3)$

	I1	TS1	I2	P1	barrier
$(H)_3C-H$	−0.7	3.8	−72.2	−61.2	4.5
$(CH_3)(H)_2C-H$	−0.7	−0.1	−72.7	−62.4	0.6
$(CH_3)_2(H)C-H$	−1.05	−1.04	−73.4	−63.4	0.01
$(CH_3)_3C-H$			−71.9	−61.9	

large number of reaction paths. The geometries and energies of the corresponding stationary points are collected in the Supporting Information. The pattern for the conformational energy of the transition states for the cases of methane, propane, and butane is similar to that reported above for ethane. In fact they all share the **alktrA** label. The alkoxy face is always preferred, and the optimal arrangement of the Tp ligand places the longest Ag−N bond in a transoid position with respect to the C5−O7 bonds. In what concerns the alkane orientation, the labeling criteria are necessarily different for each case. In methane, with three identical hydrogen substituents, there is only one rotamer of the transition state. For the case of propane, structures **TS1alktrA**, **TS1alktrB**, and **TS1alktrC** are shown in Figure 9. It can be seen that in the most stable rotamer **A**, the hydrogen substituent takes the position labeled as 13. This also happened for ethane and suggests a certain preference of hydrogen for this site. The methyl substituent seems, in contrast, to prefer position 11. The case of $(CH_3)_3$ presents the peculiarity of the existence of two rotamers despite the equivalence of the three methyl substituents. They differ in a rotation of ca. 60° around the C10−H9 chemical bond. In any case, the most stable species correspond to the roughly anti orientation of the Ag1−C5 and C10−C13 chemical bonds, which is the stable one in all other substrates, and the least stable structure will not be further discussed.

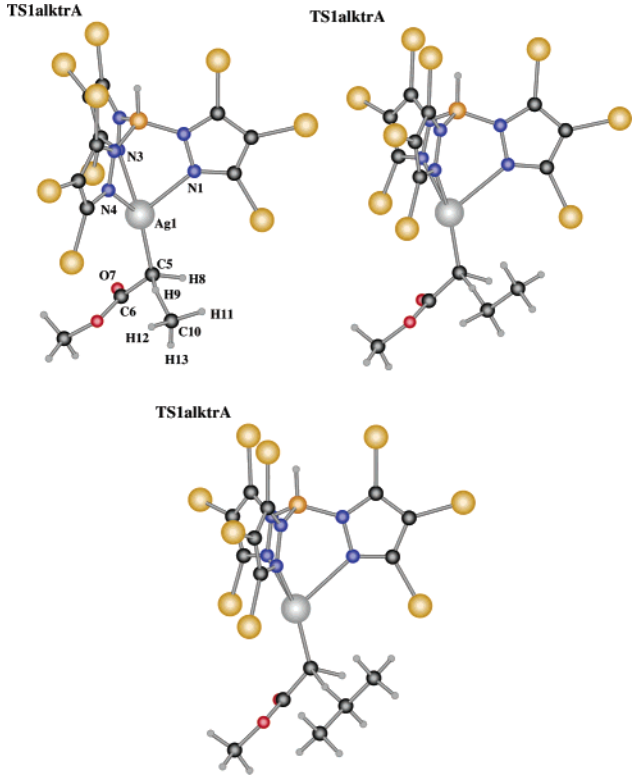

Figure 10. Transition states associated with the lowest energy pathway for C−H activation of the different alkanes by $Tp^{Br3}Ag{=}C(H)(CO_2CH_3)$.

Table 5. Selected Geometrical Parameters (Å and deg) for the Transition States Associated with the Lowest Energy Pathway for C−H Activation of the Different Alkanes by $Tp^{Br3}Ag{=}C(H)(CO_2CH_3)$

	CH_4	C_2H_6	C_3H_8
	alktrA	**alktrA**	**alktrA**
C5−H9	1.347	1.712	2.057
C10−H9	1.202	1.133	1.116
C5−C10	2.298	2.752	3.043
Ag1−C5	2.177	2.097	2.072
Ag1−N2	2.518	2.563	2.573
Ag1−N3	2.354	2.359	2.354
Ag1−N4	2.455	2.377	2.351
C5−H9−C10-X11	94.3	123.2	108.6
N2−Ag1−C5−H9	189.3	200.3	200.2
O7−C6−C5−H9	187.1	194.8	197.8
energy	3.8	−0.1	−1.04

Reactions of $Tp^{Br3}Ag{=}C(H)(CO_2CH_3)$. The carbene complex discussed above, $TpAg{=}C(H)(CO_2CH_3)$, is quite useful for theoretical studies, but is essentially a model for species $Tp^{Br3}Ag{=}C(H)(CO_2CH_3)$, which is well known experimentally as an efficient agent for C−H activation.[9] This section presents the results for the calculations on the system with the Tp^{Br3} ligand. Results on the previous section are used as a guide for the choice of the starting geometries in the search for the most stable conformation.

Table 4 presents the summary of the energetics of the C−H activation process of the different alkanes by $Tp^{Br3}Ag{=}C(H)(CO_2CH_3)$. In this case, the complete profile could be fully computed only for the first three alkanes, methane, ethane, and propane, while for butane we could not locate the transition state. This outcome can be explained by looking at the computed energies. The trend in the energy barriers shows a decrease when increasing the substitution, as observed for the systems with the Tp ligand and in agreement with experimental data. The

Table 6. Relative Energies (kcal/mol) for Stationary Points in the Lowest Energy Pathways for C−H Activation of Different Alkanes by TpCu=C(H)(CO_2CH_3) and Tp^{Br3}Cu=C(H)(CO_2CH_3)

	TpCu=C(H)(CO_2CH_3)					Tp^{Br3}Cu=C(H)(CO_2CH_3)				
	I1	**TS1**	**I2**	**P1**	barrier	**I1**	**TS1**	**I2**	**P1**	barrier
$(H)_3C-H$	−1.0	13.0	−62.9	−49.1	14.0	−0.6	10.0	−61.4	−49.8	10.6
$(CH_3)(H)_2C-H$	−1.2	8.1	−64.0	−50.4	9.3	−0.6	5.4	−61.5	−51.1	6.0
$(CH_3)_2(H)C-H$	−1.2	4.2	−63.9	−51.4	5.4	−0.7	4.0	−70.3	−52.1	4.7
$(CH_3)_3C-H$	−1.3	2.2	−63.5	−49.9	3.5	−0.6	4.0	−68.0	−50.6	4.6

Table 7. Selected Geometrical Parameters (Å and deg) for the Transition States Associated with the Lowest Energy Pathway for C−H Activation of the Different Alkanes by TpCu=C(H))(CO_2CH_3) and Tp^{Br3}Cu=C(H)(CO_2CH_3)

	TpCu=C(H)(CO_2CH_3)				Tp^{Br3}Cu=C(H)(CO_2CH_3)			
	CH_4	C_2H_6	C_3H_8	C_4H_{10}	CH_4	C_2H_6	C_3H_8	C_4H_{10}
	oxyciA	**oxyciB**	**oxyciA**	**oxyciA**	**alktrA**	**oxyciB**	**alkciA**	**alkciA**
C5−H9	1.254	1.235	1.231	1.184	1.268	1.327	1.484	1.656
C10−H9	1.280	1.299	1.312	1.398	1.258	1.223	1.180	1.154
C5−C10	2.203	2.257	2.335	2.427	2.180	2.374	2.589	2.779
Cu1−C5	1.978	1.978	1.970	1.983	1.993	1.957	1.930	1.914
Cu1−N2	2.221	2.224	2.235	2.231	2.277	2.223	2.263	2.279
Cu1−N3	2.106	2.112	2.107	2.111	2.091	2.158	2.139	2.120
Cu1−N4	2.108	2.108	2.115	2.124	2.178	2.163	2.161	2.175
C5−H9−C10−X11	150.4	218.4	99.5	100.6	98.0	218.8	85.4	53.9
N2−Cu1−C5−C6	20.8	21.7	18.9	18.2	192.4	19.2	20.1	12.1
O7−C6−C5−H9	14.5	15.1	17.7	18.8	191.9	6.6	187.9	193.5
energy	13.0	8.1	4.2	2.2	10.0	5.4	4.0	4.0

computed barrier for the case of $(CH_3)_2(H)C-H$ is as low as 0.01 kcal/mol, which in fact indicates a completely flat surface. If the barrier for the $(CH_3)_3C-H$ system has to be lower, either the process is barrierless or the potential hypersurface is so flat that our computational methods are unable to locate the transition state. The comparison of the results in Tables 2 and 4 shows that barriers are consistently lower for the case of the Tp^{Br3} ligand, therefore demonstrating the activating effect of bromine substituents.

The energetics summarized in Table 4 correspond to the lowest energy pathways. Other pathways were analyzed following the scheme explained in detail in the previous section for the system with the Tp ligand. In all cases the most stable conformer for the transition state corresponded to the same type of structure. The approach of the alkane from the alkoxy side of the carbene was always preferred, as well as the transoid arrangement of the Ag−N2 and C5−C7 bonds. The four computed transition states are shown in Figure 10, and selected geometrical parameters are collected in Table 5. The geometrical values are quite similar to those reported above in Table 3 for the TpAg=C(H)(CO_2CH_3) system. It is nevertheless noticeable that the reaction seems to be earlier for the system with the Tp^{Br3} ligand, as exemplified by the longer C5−H9 values, which is consistent with the fact that barriers are lower. The Ag−N distances are practically the same; the presence of the bromine seems to affect the electronic properties of the complex, but not the geometrical arrangement around the silver center.

Reactions of Tp^{x}Cu=C(H)(CO_2CH_3). The study reported in the previous sections on silver complexes is extended here to copper species, which had been previously reported experimentally and are known to be less active. Table 6 collects the energetics for the lowest energy pathways corresponding to the reactions of the TpCu=C(H)(CO_2CH_3) and Tp^{Br3}Cu=C(H)(CO_2CH_3) carbene complexes.

The reaction barriers for the different alkanes confirm the trend already reported for the silver complexes. The barrier decreases in the order methane > ethane > propane > butane. If we compare both copper complexes, it is clear that the general trend is that the barrier is higher for the complex with the Tp ligand than for the species with the Tp^{Br3} ligand, with the single exception of the butane species. No experimental correlation can be expected from this result because the Tp species is not likely to exist as a monomer in solution.[21] Finally, the barrier is always higher for the copper complexes than for their silver counterparts, already shown in Tables 2 and 4. All these trends are consistent with experimental expectation, thus providing further confirmation for the validity of the computed mechanism.

Selected geometrical parameters associated with the transition states of the lowest energy paths are presented in Table 7. The labels of the structures give a first indication of the significant

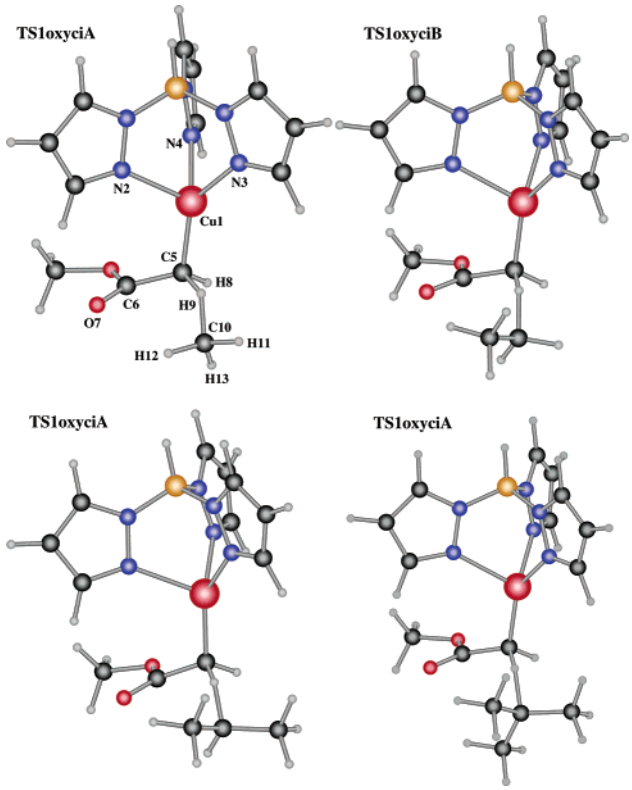

Figure 11. Transition states associated with the lowest energy pathway for C−H activation of the different alkanes by TpCu=C(H)(CO_2CH_3).

Table 8. Computed Values (kcal/mol) for the Energy Barrier Computed with (ΔE_{solv}) and without (ΔE) Solvent Effect (heptane) for the Insertion of the Carbene Group of Different Complexes in the C−H Bond of Alkanes

	$(H)_3C-H$		$(CH_3)(H)_2C-H$		$(CH_3)_2(H)C-H$		$(CH_3)_3C-H$	
	ΔE	ΔE_{solv}	ΔE	ΔE_{solv}	ΔE	ΔE_{solv}	ΔE	ΔE_{solv}
$TpCu{=}C(H)(CO_2CH_3)$	14.0	13.2	9.3	8.9	5.4	5.2	3.5	3.4
$Tp^{Br3}Cu{=}C(H)(CO_2CH_3)$	10.6	9.6	6.0	5.9	4.7	4.2	4.6	4.2
$TpAg{=}C(H)(CO_2CH_3)$	7.8	5.9	3.9	2.5	1.3	0.9	0.5	0.4
$Tp^{Br3}Ag{=}C(H)(CO_2CH_3)$	4.5	3.7	0.6	0.3	0.0	0.0		

Table 9. Computed Values (kcal/mol) for the Potential (ΔE) and Free (ΔG) Energies of the Insertion of the Carbene Group of Different Complexes in the C−H Bond of Alkanes

	$(H)_3C-H$		$(CH_3)(H)_2C-H$		$(CH_3)_2(H)C-H$		$(CH_3)_3C-H$	
	ΔE	ΔG	ΔE	ΔG	ΔE	ΔG	ΔE	ΔG
$TpCu{=}C(H)(CO_2CH_3)$	14.0	17.1	9.3	10.4	5.4	7.9	3.5	5.9
$Tp^{Br3}Cu{=}C(H)(CO_2CH_3)$	10.6	16.8	6.0	11.8	4.7	8.7	4.6	8.4
$TpAg{=}C(H)(CO_2CH_3)$	7.8	12.9	3.9	5.8	1.3	3.8	0.5	2.1
$Tp^{Br3}Ag{=}C(H)(CO_2CH_3)$	4.5	8.1	0.6	3.6	0.0	2.6		

conformational differences with the silver systems discussed above. Values around 0° in the O7−C6−C5−H9 dihedral angle, with their associated **oxy** label, are present in all reactions involving $TpCu{=}C(H)(CO_2CH_3)$ and for the reaction of $Tp^{Br3}Cu{=}C(H)(CO_2CH_3)$ with ethane. The difference can be graphically viewed in the structures shown in Figure 11. The corresponding structures through the alkoxy face, in the cases where they could be computed, had higher energy. The change in the behavior of the N2−Ag1−C5−C6 dihedral angle is even more dramatic, with seven of the eight structures having values near 0°, indicative of a cisoid arrangement of the Tp ligand. There is even one case, that of the reaction of $Tp^{Br3}Cu{=}C(H)(CO_2CH_3)$ with ethane, where the preference in the rotation of the ethyl also changes, the **B** rotamer being more stable. The conformational preferences for the copper systems seem to be much more disperse than those of the silver complexes.

If we compare the geometrical parameters for the copper complexes in Table 7 with those reported above for the silver complexes in Tables 3 and 5, there are three main differences. The reaction is more advanced at the transition state in the case of the copper complexes, as reflected in shorter C5−H9 and C5−C10 distances and longer C10−H9 distances. This is consistent with the higher barriers for copper systems. The second difference is in the metal−nitrogen distances, which are shorter for copper (values in the 2.1−2.3 Å range) than for silver (values in the 2.3−2.5 Å range) due to the smaller radius of the first-row transition metal. These shorter distances have likely steric implications and may be at the origin of the different preferences for the alkoxy/oxy faces. The third difference is in a larger dispersion in the case of copper for the values of the dihedral angles defining the conformational identities.

Free Energy and Solvation Effects. All the discussion in the previous sections has been based on gas-phase potential energies at 0 K. These are the energy parameters that are easier to compute, but do not correspond exactly to the experimentally relevant magnitudes, which are the free energies in solution. In this section we check if the trends observed in the potential energies are affected significantly by solvation and free energy effects.

Solvation effects on the energy barrier were computed through single-point PCM calculations on the structures of intermediate **I1** and transition state **TS1** for the low-energy energy paths presented above for the different systems. The solvent used was heptane because of its low dielectric constant, similar to that of the experimental solvents used often. The results are collected in Table 8, where the potential energy values are also included for comparison. Solvation effects reduce in all cases the energy barrier, by a value between 2.9 and 0.1 kcal/mol. This reduction means that the transition state is better solvated. The relevant result for this work is that the trends in the values for energy barriers are completely unchanged by solvation effects. The barriers always decrease in the sequence methane > ethane > propane > butane. The sequence TpCu > $Tp^{Br3}Cu$ > TpAg > $Tp^{Br3}Ag$ is also conserved with the same single exception for the reaction between copper complexes and the butane system discussed above.

Free energy corrections were computed in an analogous way through single-point frequency calculations. The free energy correction includes zero-point energies, as well as thermal and entropic contributions. Zero-point energy corrections have very little effect on the energy barriers; a table with the specific values is included in the Supporting Information. The results are collected in Table 9, along with the potential energy values. The free energy corrections involve in all cases an increase in the barrier, by a value between 6.2 and 1.6 kcal/mol. The increase in the barrier is consistent with the fact that transition state **TS1** is more organized than the loosely bound intermediate **I1**. The formation of **TS1** has thus an entropic penalty, and this is reflected in the ΔG value. Despite the fact that free energy corrections are larger than solvation effects, the main overall trends are also conserved. In all cases, the sequence concerning the alkane substrates is conserved. As for the sequence concerning the metal fragment, the trends between silver and copper systems and between both silver complexes are conserved. Free energy corrections do alter the ordering between the TpCu and $Tp^{Br3}Cu$ complexes for the cases of ethane and propane. This means that the entropic penalty in the more crowded $Tp^{Br3}Cu$ system is able in particular cases to offset the electronic advantage of the presence of the bromine substituents. Again, this inversion is not critical because of the dimeric nature of the TpCu complex in solution.[21]

If we were to consider the combined effect of solvation and free energy effects, we would find that they go in opposite directions and that they are dominated by the free energy term, which is consistently larger. In any case, the overall trends observed in the potential energies are essentially maintained when solvation and free energy contributions are taken into account. A reasonable prediction on selectivity can therefore be obtained from potential energy calculations, which are easier to carry out.

(21) Mealli, C.; Arcus, C. S.; Wilkinson, J. L.; Marks, T. J.; Ibers, J. A. *J. Am. Chem. Soc.* **1976**, *98*, 711.

Table 10. Computed Values (kcal/mol) of the Energy Barrier for the Insertion of the Carbene Group of Different Complexes in the C−H Bond of Different Alkanes

	$(H)_3C-H$	$(CH_3)(H)_2C-H$	$(CH_3)_2(H)C-H$	$(CH_3)_3C-H$
TpCu	14.0	9.3	5.4	3.5
$Tp^{Br3}Cu$	10.6	6.0	4.7	4.6
TpAg	7.8	3.9	1.3	0.5
$Tp^{Br3}Ag$	4.5	0.6	0.0	

Discussion

The main result of the calculations is the summary of potential energy barriers collected in Table 10. Two trends are clearly defined. Activation is increasingly easier in the sense methane < ethane < propane < butane, without any exception. As for the activity of the metal fragments, the order is TpCu < $Tp^{Br3}Cu$ < TpAg < $Tp^{Br3}Ag$, with very few exceptions. These results follow faithfully the previous experimental suggestions. On one hand, this lends support to the validity of our proposed reaction mechanism, with the insertion taking place in a concerted step with a low energy barrier. On the other hand, this further confirms the generality of the trends, which could not be experimentally evaluated in a systematic way for all systems considered here, the methane substrate being a typical example.

The computational reproduction of the experimentally suggested trends lends support to the qualitative explanations that had been given before. As far as the alkane species is concerned, the key factor is the strength of the C−H bond. The insertion of the carbene into the C−H bond implies the homolytic cleavage of the latter. The facility of the alkane to undergo this process thus rules its reactivity. For the trends related to the metal fragment, the key factor is its back-donating ability, which can be experimentally characterized by the ν(CO) frequency of the related carbonyl species. The highest frequencies correspond to the less back-donating metal fragments, which will in turn produce the more reactive carbenes. Ag is more electropositive than Cu, and thus Ag complexes are more efficient. The bromine substituents of Tp^{Br3} have better electron-accepting abilities than the hydrogen substituents of Tp, thus making the systems with the brominated ligand more reactive.

It is worth pointing out that the kinetic trends derived from the computed energy barriers are not in full agreement with the thermodynamic trends that could be deduced from the relative energies of products **P1** presented throughout the paper for the different reactions. For the alkane systems, the thermodynamic stabilities of the products would indicate the following ordering of reactivity: methane < butane < ethane < propane. For the butane system, with its tertiary C−H bond, the reaction is less exothermic than for ethane or propane. This is likely related to steric effects related to the presence of three ethyl groups, but these steric effects are still not apparent in the early transition state of the reaction. In the case of the metal fragments, the thermodynamics would suggest the following order of reactivity: TpCu < $Tp^{Br3}Cu$ < $Tp^{Br3}Ag$ < TpAg. This is in disagreement with the experimental observation that the bromine substituents in tris-pyrazolylborate favor the reactivity of the complex. These types of reactions are thus under kinetic control, and no deductions on the selectivity can be made on the basis of the relative stabilities of the products.

The calculations show that a variety of competing pathways related to conformational rearrangements of the transition state are available for each system. With data available on four different systems, we can try to identify general trends on the relative energies of the transition states in order to simplify the conformational analysis on future studies. No general rule seems possible for the region of approach of the alkane to the carbene. The alkoxy face is always preferred when the metal is Ag, but the copper systems present examples of either alkoxy or oxy faces. The reasons are not clear, and therefore it is advisable to test both faces for each new set of metal and Tp ligand. The arrangement of the M−N bonds of the Tp ligand seems to be less complex. The arrangement labeled as transoid is always favored for the attack through the alkoxy face, while the cisoid conformation is usually preferred for the oxy face, although there are some exceptions. This can cut the computational effort involved in the conformational search by nearly half. The position of the alkane substituents, in what has been labeled as **A**, **B**, and **C** isomers depends on the particular alkane being studied, but a preference is nevertheless visible for certain rotamers. In particular, hydrogen substituents seem to prefer the position we have labeled as 13, while methyl substituents occupy positions 11 and 12. The differentiation between positions 11 and 12 is not very clear, and different rotamers have to be evaluated in case of doubt.

Conclusions

The reaction mechanism for the activation of the C−H bond of alkanes by metallocarbene complexes $Tp^xM{=}C(H)(CO_2CH_3)$ (Tp^x = Tp, Tp^{Br3}; M = Cu, Ag) has been clarified with the help of DFT calculations. The alkane forms first a weak van der Waals complex with the metallocarbene, which evolves toward products through a low-barrier transition state where M−C and $H-C_{alkane}$ bonds are broken and C−C and $H-C_{carbene}$ bonds are formed in a concerted way. The selectivity of the process is under kinetic control and decided precisely by the energy of this transition state. The tris-pyrazolyl ligand remains bound to the metal in a tridentate fashion throughout the whole reaction.

Examination of the reaction for different combinations of metallocarbene complexes and alkanes shows clear trends in the energy barriers. The facility to activate C−H bonds increases in the order methane C−H < primary C−H < secondary C−H < tertiary C−H. The reaction is easier when the metal is Ag than when it is Cu, and the use of the Tp^{Br3} ligand favors the reaction with respect to the use of Tp. These trends confirm previous suggestions from the experimental observations. In fact, they reinforce these suggestions because the range of systems amenable to calculation is larger due to the absence of competing reactions in our computational models.

A number of competing paths have been identified for each C−H bond activation process. They are related to conformational flexibility in the transition state, in particular to the direction of approach of the alkane, its orientation, and the arrangement of the metal−nitrogen bonds. The calculations allow a better understanding of the factors affecting the nature of the most stable conformer. These observations will be used in the design of future computational studies on different combinations of alkane and metallocarbene systems that will be undertaken in our laboratory.

Acknowledgment. Financial support from the Spanish MEC (projects CTQ2005-09000-CO1-02/BQU, CTQ2005-00324/BQU, Consolider Ingenio 2010 CSD2006-0003), the Catalan DURSI (project 2005SGR00715), and the ICIQ Foundation is acknowledged.

Supporting Information Available: PDF file containing the full ref 14, a table with the barriers corrected by zero-point energies, and information (Cartesian coordinates, total energy) on the structures reported in the text. This material is available free of charge via the Internet at http://pubs.acs.org.

OM060445H